

Experimental and Theoretical Analysis of the Vibrational Spectra and Theoretical Study of the Structures of 3,6-Dichloropyridazine and 3,4,5-Trichloropyridazine

J. Vázquez,*† J. J. López González,† F. Márquez,† G. Pongor,‡ and James E. Boggs§

Department of Physical and Analytical Chemistry, University of Jaén. E-23071, Jaén, Spain, Department of Theoretical Chemistry, Eötvös Loránd University, P.O. Box 32, H-1518 Budapest 112, Hungary, and Institute for Theoretical Chemistry, Department of Chemistry and Biochemistry, University of Texas, Austin, Texas 78712

Received: September 10, 1999; In Final Form: December 8, 1999

The infrared and Raman spectra of 3,6-dichloropyridazine and 3,4,5-trichloropyridazine were recorded. These spectra were taken in the solid phase and with various solvents (HCCl₃, CS₂, CCl₄), giving wavenumbers and relative intensities of the bands and the qualitative Raman depolarization ratios. Conventional ab initio methods at the Hartree–Fock and MP2 levels using the 3-21G*, 6-31G*, 6-31G**, and 6-311G** basis sets, as well as density functional theory (DFT) using the 6-31G* basis functions and the BLYP and B3LYP functionals, were used to predict the geometries and to calculate the harmonic frequencies and force fields of these molecules. In addition, coupled cluster calculations, i.e., CCSD and CCSD(T), using the 6-311G** basis set were included to evaluate the geometries of pyridazine and 3,6-dichloropyridazine, analyzing in detail the structure of these systems. To fit the calculated wavenumbers to the experimental ones, the B3LYP/6-31G* force field was selected to be scaled. The following two sets of scale factors were tested: (1) a standard set derived from a training set of 30 organic molecules (*set A*), and (2) a set directly calibrated from the pyridazine molecule (*set B*). The calculations indicate that pyridazine and its chlorinated derivatives show less aromatic character than expected. The B3LYP exchange–correlation functional with the 6-31G* basis functions gave the most reliable structural parameters for both molecules. The a priori scaled spectra were sufficiently decisive to get a complete assignment of the vibrational spectra. Both series of scale factors led to similar results. However, although the standard set (*set A*) proved to be an useful tool to carry out the initial assignments, further detailed analysis of the spectra required specific empirical parameters derived from the pyridazine molecule. This was especially true for the most congested spectral areas.

I. Introduction

Throughout the past century, the diazines have been among the most studied heterocyclic compounds.¹ For many years, attention has been paid to pyrimidines and pyrazines, the former because they are of great importance in fundamental metabolism: uracil, thymine, and cytosine are three of the six bases found in the nucleotides, and thymine and cytosine two of the four crucial bases in nucleic acids.² The pyrimidine ring also occurs in the vitamin thiamin.² The pyrazines, for example, turn up in the fungal metabolite aspergillidic acid and, more interestingly, as a 1,4-dihydropyrazine in the luciferin of *Cypridina hilgendorffii*, responsible for the chemiluminescence of this ostracod.³ By contrast, no naturally occurring pyridazine compound is known. Moreover, the 1,2-diazine shows a low vapor pressure and an abnormally high boiling point which, at 207°, is 80°–90° higher than that of any of the other simple azines.⁴ Both effects are due to the polarizability of the N–N system in pyridazine, which results in extensive dipolar association in the liquid. Only recently have the therapeutic potential⁵ and other medical and technological applications⁶ of

pyridazine derivatives been pointed out. Thus pyridazines would now seem to deserve intensive fundamental investigation, as has been done for the pyrimidines and pyrazines.

Unsubstituted diazines are more resistant to electrophilic substitution than, e.g., pyridine, so the most important aspect in the chemistry of this series involves reactions with nucleophilic reagents. In diazines, the second nitrogen helps by generating electron deficiencies at atoms on which negative charge builds up during a nucleophilic reaction involving the first nitrogen atom.¹ In reactions with nucleophilic reagents, the relative ease of nucleophilic displacement of halogens is generally observed, with the chlorine atom most commonly used. Thus the chlorinated derivatives of the three diazines are taking an increasing role as precursors in many synthetic routes seeking pharmacologically useful products.⁷

It is therefore not surprising to find extensive information and, in particular, vibrational analysis about chloropyrimidines⁸ and chloropyrazines,⁹ although such accurate information does not yet exist for chloropyridazines. Specifically, only a few previous studies exist dealing with the structure^{10,11} and vibrational¹² and electronic¹³ spectra of 3,6-dichloropyridazine. Unfortunately, in the previous experimental vibrational studies, we can prove that the reported spectra showed a high percentage of impurities, which led to a completely mistaken assignment of the spectra. In particular, approximately the 70% of the analyzed bands belonged to a decomposition product of dichloropyridazine.

* Author to whom correspondence should be addressed. Fax: 34-953-212526; e-mail: jvazquez@ujaen.es.

† University of Jaen. Fax: 34-953-212526. E-mail: jvazquez@ujaen.es.

‡ Eötvös Loránd University. Fax: 36-1-2090602. E-mail: pongor@para.chem.citc.hu.

§ University of Texas. Fax: 512-471-8696. E-mail: james.boggs@mail.utexas.edu.

TABLE 1: Observed Infrared Wavenumbers (cm⁻¹) for 3,6-Dichloropyridazine^a

KBr		Nujol		fluorolube		HCCl ₃		CCl ₄		CS ₂		polycryst.	
ν	<i>I</i>	ν	<i>I</i>	ν	<i>I</i>	ν	<i>I</i>	ν	<i>I</i>	ν	<i>I</i>	ν	<i>I</i>
3116	s	3115	w	3115	w	3120	m	3119	m	3118	m	3116	s
3098	m	3098	vw	3100	sh	3105	w					3099	m
3067	s	3066	w	3065	w	3072	m	3071	m	3071	m	3067	s
3052	w	3051	vw	3051	sh							3052	m
3042	m	3040	w	3040	vw	3045	m	3045	m	3045	m	3043	m
2922	vw			2922		2922	vw			2926	vvw	2925	w
2853	vvw					2853	vvw					2854	vw
2819	vvw			2819	vvw	2819	vvw	2819	vvw	2817	vvw	2819	vw
2760	vvw	2758	vvw			2767	vvw	2760	vvw	2762	vw	2764	vw
2691	vw	2691	vvw			2692	vw	2688	vw	2688	vw	2688	w
						2665	vvw	2662	vvw	2662	vw	2663	vw
2593	vvw	2593	vvw			2589	vvw	2585	vvw	2588	vvw	2590	vw
2540	vw	2540	vvw			2542	vw	2536	vw	2536	vw	2538	w
								2514	vvw				
2463	vvw							2453	vvw	2458	vvw	2463	vw
												2360	vvw
2326	vw	2326	vvw			2323	vvw	2323	vw			2324	vvw
						2315	vvw						
2303	vw	2303	vvw	2303	vvw	2304	vvw	2303	vw			2302	w
2196	vw	2195	vvvw	2195	vvw	2197	vvw	2192	vw			2194	w
2170	vvw					2165	vvw	2165	vvw			2165	vvw
2061	vvw					2066	vvw	2061	vvw			2061	vvw
1961	vw	1960	vw	1960	vvvw							1960	w
						1947	vw	1942	vw	1940	vw		
1927	vvw					1923	vvw	1918	vvw				
1850	vvvw					1850	vvw	1850	vvw	1849	vvw	1849	vvw
1816	vvvw	1816	vvvw			1802	vvw	1808	vvw	1802	vvw	1802	vvw
1739	vvw												
												1684	w
1674	vw	1677	vw	1670	vvw			1669	vvw			1670	w
1662	vw	1662	vw			1666	vw			1661	vw		
1591	w	1590	w	1591	vvw	1588	w					1586	m
1556	s	1555	s	1554	m	1556	s					1551	s
1528	s	1527	s	1527	m	1527	s					1528	s
1515	vw	1515	vw	1507	vvw	1517	m			1517	vvw	1515	vw
1491	vw					1491	vvw					1498	vw
1472	vw												
1408	m	1408	w	1408	vvw	1408	m	1404	m	1405	s	1407	m
1387	vs					1385	vs	1382	vs	1383	vs	1385	vs
1379	vs											1380	sh
												1350	sh
1299	w	1299	vw			1296	w	1297	vvw	1297	w	1299	w
1286	vw											1279	vvw
1246	w	1247	sh									1247	vw
1168	s	1168	m									1167	m
1159	s	1148	m									1151	vs
1147	vs	1140	s			1144	vvs	1142	vs	1137	vs	1141	vs
1129	vs	1129	s			1126	vs					1131	vs
												1108	w
1062	vvw					1062	vvw	1062	vvw	1062	vvw	1060	vw
1045	s	1044	m			1043	s	1043	s	1043	s	1044	s
1035	m	1035	w			1035	m	1032	m	1031	m	1030	s
1019	m	1015	w					1012	w	1012	vvw	1016	w
983	w											984	w
927	vvw											927	vvw
915	w									910	vvw	915	vw
902	vw											904	vvvw
848	sh												
836	s	836	s	836	m	833	s	832	s	832	s	840	s
806	w											805	w
780	s	782	s	782	m							782	s
741	vw	741	vw									741	vvw
628	m	628	m	628	w					628	m	628	w
555	s	555	s	555	m	555	s	554	s	555	s	555	s
552	s	551	s	551	m	552	s	551	s	551	sh	552	s
507	w	507	w	507	vw	506	vvw	502	vvw	502	vw	507	w
403	vvw	407	vw										
		392	vvw										
		372	w, br										
		347	vvw										
		343	vvw										
		298	vw										

^a Abbreviations: *I*, relative intensity; s, strong; m, medium; w, weak; v, very; br, broad; sh, shoulder.

TABLE 2: Observed Infrared Wavenumbers (cm⁻¹) for 3,4,5-Trichloropyridazine^a

KBr		Nujol		fluorolube		HCCl ₃		CCl ₄		KBr		Nujol		fluorolube		HCCl ₃		CCl ₄	
<i>ν</i>	<i>I</i>	<i>ν</i>	<i>I</i>	<i>ν</i>	<i>I</i>	<i>ν</i>	<i>I</i>	<i>ν</i>	<i>I</i>	<i>ν</i>	<i>I</i>	<i>ν</i>	<i>I</i>	<i>ν</i>	<i>I</i>	<i>ν</i>	<i>I</i>	<i>ν</i>	<i>I</i>
				3122	vw									1813	w	1818	w	1812	w
3104	vvw	3069		3104	vvw									1795	w				
3069	m	3063	sh	3069	s, sh			3070	s					1773	w				
3063	s		w	3062	s	3064	m							1676	w				
				3044	sh									1521	w				
3032	m	3032	vw	3030	m			3028	w	1526	sh								
3007	m	3007	w	3006	m	3009	s	3004	w	1519	vs	1518	vs						
2986	w			2983	w					1512	sh	1512	s,sh						
				2972	w					1498	s	1498	vs	1498	vs				
2926	w									1457	br, sh			1465	w				
2901	w			2902	w	2895	w	2894	w	1382	s			1380	vs				
				2887	w	2870	w	2870	w	1336	vvw	1335	vw						
2878	w			2876	w					1293	vs	1292	s						
2761	vvw			2761	vw	2754	vvw	2761	w	1267	vs	1267	vs						
2727	vvw	2729	w	2729	vw	2721	vvw	2722	w	1263	vs								
2704	vvw									1245	sh					1240	m	1242	s, sh
2669	vw	2669	w	2671	vw	2665	w	2665	w	1210	s	1210	s			1207	vs	1207	vs
				2619	vvw	2613	vw			1179	m	1179	s			1174	s	1169	s
2589	vvw			2590	vvw	2587	vw			1095	vw	1095	w			1095	m	1095	m
2566	vw	2566	w	2558	w	2551	w	2551	w	1034	vs	1033	vs			1032	vs	1032	vs
2528	vvw			2529	vw	2531	vw			960	vvw								
2464	vvvw			2465	sh	2451	vw			938	w	938	m			941	m		
2436	vvvw			2419	sh			2427	w	931	m	931	m					931	w
2347	vvvw	2349	w									907	w			910	s	909	s
		2274	w			2266	vw	2261	w	854	m	854	w						
2219	vw	2219	w			2213	w	2209	w	826	vvs	827	vs			829	vs	827	vs
2188	vvw					2193	vw			817	sh	817	sh						
						2148	vvw			798	sh	798	sh						
				2123	vw	2121	vvw			770	s	770	s						
				2097	vvw	2092	vvw			738	vw	738	w						
				2052	w	2046	w	2049	w	547	s	547	s			546	s	545	s
				2035	vw	2039	w	2036	w	526	w	524	w			523	m	522	m
				2003	vvw					509	s	508	s			506	s	505	s
				1981	vvw	1975	vw			485	br, sh							458	vw
						1920	vvw			413	w	413	w			412	w	411	w
						1877	vw					344	vw						
				1865	m	1862	w	1859	w	269	w	265	w	265	w	265	w	267	w
										223	m	220	m	220	m	220	m	221	m

^a Abbreviations: *I*, relative intensity; s, strong; m, medium; w, weak; v, very; br, broad; sh, shoulder.

In view of the growing importance of the chlorinated derivatives of pyridazine and the lack of knowledge of their structural parameters and vibrational behavior, in this work our aim has been to study the structure and vibrational spectrum of 3,6-dichloropyridazine and 3,4,5-trichloropyridazine. Their infrared and Raman spectra in different phases have been recorded. Theoretically, their geometries and vibrational wavenumbers were first determined by quantum mechanical calculations at the HF/3-21G*, HF/6-31G*, HF/6-31G**, MP2/6-311G**, BLYP/6-31G*, and B3LYP/6-31G* levels. The geometries were also evaluated, at the CCSD/6-311G** and CCSD(T)/6-311G** approximations for pyridazine and at the CCSD/6-311G** level for 3,6-dichloropyridazine. Next, the assignment of their vibrational spectra was accompanied by calculations of scaled B3LYP/6-31G* quantum mechanical force fields obtained by using either a series of standard scaling factors derived in the previous literature¹⁴ or a set of parameters (scale factors) whose values were previously calibrated from the pyridazine molecule. The a priori calculated spectra were decisive in the assignment of the complete set of fundamentals.

II. Experimental Section

Commercial 3,6-dichloropyridazine (97%, Aldrich) and 3,4,5-trichloropyridazine (97%, Fluka), both in the solid phase at room temperature, were purified by repeated distillation in a vacuum until the Raman spectra did not show any impurity. The solvents

used were CCl₄ (99% (GC), Panreac), HCCl₃ (99.85%, Aldrich), and CS₂ (99%, Aldrich). Mineral oil mulls were prepared with Nujol (paraffin oil) (Aldrich) and Fluorolube (Hooker Chemical Corporation, Perkin-Elmer Corp. No. 186-2301). KBr (for spectroscopy, Panreac) was used for spectra in alkaline halide pellets. All the spectra were recorded at room temperature.

Raman spectra (70–3500 cm⁻¹) were measured with a Bruker RFS 100 Fourier transform (FT) Raman spectrometer with a cooled Ge detector at liquid nitrogen temperature and a beam splitter of quartz. Radiation of 1064 nm from an air-cooled, diode-pumped Nd:YAG laser (Spectron Laser Systems) for excitation with a bandwidth of 0.5 cm⁻¹ was used. A back-scattering (180°) configuration, an acquisition mode of double-side forward–backward, and an optical retardation velocity of 1.60 cm × s⁻¹ were fixed. The spectral resolution was 1 cm⁻¹ using a Blackman-Harris four term apodization function. The laser power at the samples was 100 mW and 80 mW for samples in solution and in the solid phase, respectively. Between 300–400 scans were accumulated using a quartz cell of 5 mm length for liquid samples and an aluminum cylindrical holder (2 mm radius × 4 mm length) for solid samples. Polarization spectra were also recorded under the same conditions. For collection of the parallel and perpendicular components of the polarized Raman spectra of solution samples, a polarizer was placed in the scattered beam, and two measurements were carried out with the polarizer transmitting along directions parallel and perpen-

TABLE 3: Observed Raman Wavenumbers (cm⁻¹) for 3,6-Dichloropyridazine^a

solid			HCCl ₃			CCl ₄			CS ₂			solid			HCCl ₃			CCl ₄			CS ₂				
$\Delta\nu$	<i>I</i>		$\Delta\nu$	<i>I</i>	pol	$\Delta\nu$	<i>I</i>	pol	$\Delta\nu$	<i>I</i>	pol	$\Delta\nu$	<i>I</i>		$\Delta\nu$	<i>I</i>	pol	$\Delta\nu$	<i>I</i>	pol	$\Delta\nu$	<i>I</i>	pol		
3117	s		3121	s	p	3120	s	p	3117	s	p	1226	vw												
3100	m		3106	m	dp	3105	m, sh	dp	3102	m, sh	dp	1185	m	1183	m	p	1181	m, sh	p	1183	m	p			
3068	s		3073	s	p	3072	s	p	3070	s	p	1168	vvs	1166	s	p	1165	s	p	1163	s	p			
3052	m		3056	m	dp	3054	m	dp	3052	m	dp	1164	vs, sh												
3043	m		3047	m	p	3047	m	p	3045	m	p	1151	m	1154	sh	p	1153	sh		1151	sh	p			
2970	vvw											1141	s	1141	m	p	1140	m	p	1138	m	p			
2966	vw					2949	vw					1126	w, sh	1129	sh	p	1126	sh	p	1123	w	p			
2922	vw		2929	vw	dp	2930	w		2917	w	p	1109	w	1109	w	p	1107	w							
2903	w		2906	vw	p	2907	w		2901	w	p	1087	s	1087	vw		1087	vvw							
2759	vvw											1064	w	1064	vvw		1064	vw, sh							
2710	w		2714	vw		2711	vvw					1044	s	1044	m	p	1043	m	p	1043	m	p			
2687	vw		2690	vw		2691	vvw					1036	m	1035	sh		1032	sh	dp	1030	sh, br	dp			
2542	vvw											1017	w												
2464	w		2462	vw		2459	vvw										992	vvw							
2439	vw		2436	vw		2432	vvw					984	w	977	vvw										
2338	vw		2338	vw		2333	vvw					836	w												
2306	vvw											816	m	816	m	p	813	w, sh		812	sh	p			
2294	vvw											781	vvs	780	vs	p	780	s	p						
2273	vvw											742	m												
2210	vw		2207	vw								713	w				714	vvw							
2186	vvw											698	vw				695	vvw							
2157	vvw		2158	vvw								671	vw												
2075	vvw		2073	vvw								634	m												
1944	vvw		1945	vw		1936	vvw					628	s	631	s	dp	630	m	dp	630	m	dp			
1820	vvw		1815	vvw		1899	vvw					596	vw												
1750	vvvw											557	w	553	w, sh	dp	554	w, sh	dp						
1683	vvw		1682	w		1684	vw					554	sh	507	w	dp	551	vw	dp						
			1586	vvw	dp	1586	sh		1586	vvw		508	w				504	w	dp						
1555	s		1556	vs	dp	1556	s	dp	1555	s	dp														
1552	sh		1539	sh		1539	sh																		
1528	m		1530	m	dp	1530	m	dp	1528	m	dp	407	w	402	w, br										
1516	w		1518	w	dp	1518	sh		1518	sh		373	w				374	w	dp	375	w	dp			
1495	vw		1495	vw		1495	vw		1495	vw		349	vvs	349	vvs	p	348	vs	p	348	vs	p			
1483	w		1483	w	p	1482	vvw	p	1481	w	p	345	vs	345	vs	p	344	s	p	345	s	p			
1437	vw											341	sh												
1394	vw		1392	vw								299	s	296	m	dp	297	m	dp	296	m	dp			
1387	vw, br		1388	vw	dp	1387	vw, br	dp				283	m				282	sh							
			1332	vvw								243	vvw												
1299	w, br		1298	w	p	1297	vw		1296	w		232	w	235	vvw										
1261	w		1261	w		1259	vvw		1257	vvw		156	w				154	vvw	vvw						
												114	sh	116	sh	sh	115	sh	sh						

^a Abbreviations: *I*, relative intensity; s, strong; m, medium; w, weak; v, very; br, broad; sh, shoulder; p, polarized; dp, depolarized.

dicular, respectively, to the polarization direction of the laser beam. The observed depolarization ratio (ρ) varied from 0 to 0.75. For this experimental configuration, $\rho < 0.75$ for the totally symmetric vibrations,¹⁵ referred to as polarized bands. For modes that do not belong to the totally symmetric representation, $\rho \approx 0.75$; these bands are depolarized.

The infrared spectra in the 400–4000 cm⁻¹ range were recorded using a Perkin-Elmer 1760-x FT-IR spectrometer equipped with a Globar source, a Ge/KBr beam splitter and a (triglicinesulfate) TGS detector. Also, the 200–4000 cm⁻¹ range was recorded with a Bruker Vector 22 FT-IR spectrometer with a high-intensity Globar source, a CsI beam splitter and a deuterated triglicinesulfate (DTGS) detector. The instrument was calibrated by using an indene–camphor–cyclohexane mixture (1:1:1). The interferogram was typically sampled to give 1 or 0.5 cm⁻¹ resolution using a Blackman-Harris three-term apodization function, a double-sided acquisition mode, and an optical retardation velocity of 1.6 cm × s⁻¹. Water and carbon dioxide were removed from the optical path by subtracting the background from the sampled spectrum. The IR spectra in solution were taken with a Perkin-Elmer 186-0091 liquid cell using KBr and CsI windows and a Beckman 199051 cell with CsI windows. KBr pellets and Nujol and Fluorolube mulls were used for solid samples. The mulls were prepared using the liquid

cells described above. In addition, for 3,6-dichloropyridazine the solid-phase spectrum was also obtained by condensing the sample on a liquid cell fitted with KBr windows by previously melting the solid at 70 °C. The sample was condensed as an amorphous solid.

All the observed infrared bands are listed in Table 1 and Table 2 for 3,6-dichloropyridazine and 3,4,5-trichloropyridazine, respectively. The Raman experimental information is collected in Tables 3 and 4 for the di- and trichlorinated derivatives, respectively. Examples of the IR and Raman spectra recorded for each studied molecule are shown in Figure 1 for 3,6-dichloropyridazine and in Figure 2 for 3,4,5-trichloropyridazine.

III. Method and Details of Calculation

Fully optimized geometries of both chlorinated molecules, as well as the vibrational wavenumbers and force constants of 3,6-, 3,4,5-chloropyridazine and pyridazine, were obtained using two quantum mechanical approaches: (1) conventional ab initio methods at the LCAO–MO–SCF-restricted Hartree–Fock¹⁶ level and Møller–Plesset perturbation theory¹⁷ of the second order (MP2), applying the frozen-core (fc) approximation;¹⁶ and (2) density functional theory methods in the Kohn–Sham formulation,¹⁸ where the calculations were carried out twice,

TABLE 4: Observed Raman Wavenumbers (cm⁻¹) of 3,4,5-Trichloropyridazine^a

solid		HCCl ₃			CCl ₄			CS ₂			solid		HCCl ₃			CCl ₄			CS ₂			
$\Delta\nu$	<i>I</i>	$\Delta\nu$	<i>I</i>	pol	$\Delta\nu$	<i>I</i>	pol	$\Delta\nu$	<i>I</i>	pol	$\Delta\nu$	<i>I</i>	$\Delta\nu$	<i>I</i>	pol	$\Delta\nu$	<i>I</i>	pol	$\Delta\nu$	<i>I</i>	pol	
3184	vvw										1330	vvvw				1314	vvw					
3166	vvw										1315	vvvw										
3098	sh	3075	s	p	3074	s	p	3071	s	p	1294	vvw	1294	vw		1295	vw		1292	vw		
3070	s										1265	w	1264	vvw		1267	vw	dp	1266	w	dp	
3065	s										1242	w	1234	vvw		1236	vw		1237	vw		
3045	w										1212	s	1208	vs	p	1208	vs	p	1207	vs	p	
3033	m				3027	m	p	3027	m	p	1180	vs	1174	vs	p	1170	vs	p	1169	vs	p	
3008	m				3006	m	p	3003	m	p	1156	sh										
2990	sh				2985	vvw					1113	vvvw										
2930	vw										1093	s	1097	m	p	1095	m	p	1095	m	p	
2903	w	2895	vw		2895	w		2890	w		1087	m	1088	vvvw		1089	sh, vw					
2881	w	2871	vw		2850	w		2865	vvw		1071	vvw	1070	vvvw		1069	vvw					
2848	vvw										1046	vw										p
2818	vvw										1035	s	1033	m	p	1033	m	p	1032	m	p	
2766	vw	2762	vvvw								982	vw				973	vvvw					
2727	vw	2724	vvvw		2727	vvw					932	vw										
2695	vw	2687	vvvw		2672	vvw							916	vvw	dp	911	vvw	dp	909	vvw	dp	
2670	vw										826	w	830	vvw		828	vvw		828	sh		
2591	vw	2583	vvvw		2581	vvw		2581	vvw		796	w										
2565	vvw	2555	vvw		2559	vvw					770	m	768	m	dp				767	m	dp	
2530	vvvw	2528	vvw		2529	vvw		2524	vvw		738	w										
2479	vvvw										713	vvw										
2437	vvvw										610	vvw				614	vvw					
2418	vvw	2404	vw	p	2404	vw	p	2402	vvw	p	546	w	546	w	p	546	w	p	544	sh		
2351	vw	2345	vw	p	2331	vw	p	2328	vvw	p	539	w										
2307	vvw										526	m	522	s	p	522	s	p	520	s	P	
2266	vw	2263	vw	p	2266	vw	p	2261	vvw	p	507	vvs	504	vs	p	503	vs	p	502	vs	p	
2221	vw										443	vw										
		2210	vw	p	2208	vw	p	2209	vvw	p	414	s	412	s	dp	412	s	dp	412	s	dp	
								2190	vvw	p	368	w										
1649	vvw										348	s	349	s					349	s	dp?	
1596	vvw	1584	vw		1588	vw, br					282	w										
1525	sh										271	m							264	vw		
1520	s	1522	s	dp	1521	s	dp	1520	s	dp	226	s										
1499	s	1499	s	dp	1498	s	dp	1497	s	dp	217	s							210	vs	dp	
1476	w	1477	w	p	1477	w	p	1476	w	p	211	s	210	vs	dp				205	vs	dp	
1465	vvw										202	s	202	vs	dp				202	vs	dp	
1438	vvvw	1440	w, br		1439	vvw					156	vw										
1414	vvvw				1415	vvw					112	vs										
1391	sh										106	sh		dp								
1384	m	1380	m	dp	1380	m	dp	1380	m	dp	81	sh	94	s, sh		92	s, sh	dp				
1348	vvvw	1330	vvw		1333	vvw																

^a Abbreviations: *I*, relative intensity; s, strong; m, medium; w, weak; v, very; br, broad; sh, shoulder; p, polarized; dp, depolarized.

using the following: (1) Becke's exchange functional¹⁹ in combination with the Lee, Yang, and Parr (LYP) correlation functional²⁰ (BLYP), and (2) a hybrid Becke's three-parameter exchange functional²¹ in combination with the LYP correlation functional (B3LYP). This hybrid HF–DFT functional introduces a percentage of the "exact" Hartree–Fock exchange term in the density functional. With each method, a series of standard split-valence basis sets was used, i.e., 3-21G*,²² 6-31G*,²³ and 6-31G**²⁴ in the HF level, 6-31G* in the DFT approximation methods, and 6-311G**²⁵ with the MP2 treatment. The geometries of pyridazine and 3,6-dichloropyridazine were calculated by coupled cluster theory, using single and double excitation (CCSD)^{26,27} and the 6-311G** basis set. The structure of pyridazine was also evaluated using the coupled cluster method with single and double excitation plus quasi-perturbative triple excitation (CCSD(T))^{26,28} and the same basis set. The structures corresponding to the minimum of energy with respect to displacement of the nuclear coordinates were obtained by the simultaneous relaxation of all geometric parameters using the gradient method of Pulay.²⁹ The Hartree–Fock, MP2, BLYP, and B3LYP quantum chemical calculations were performed using the GAUSSIAN 92³⁰ and GAUSSIAN 94³¹ packages. The CCSD and CCSD(T) calculations were carried out by the ACES

II program system.³² The new theoretical contributions to the geometry parameters, along with part of the previous available experimental and theoretical data, are listed in Table 5 for pyridazine and 3,6-dichloropyridazine and in Table 6 for 3,4,5-trichloropyridazine.

The vibrational wavenumbers and force constants were calculated from analytic first and second derivatives of the potential energy. The next goal was to derive appropriate scaled quantum mechanical force fields for these chlorinated derivatives which would be useful to assign their vibrational spectra.

Rauhut and Pulay,¹⁴ using the B3LYP/6-31G* and BLYP/6-31G* force fields of 31 organic molecules containing the atom of C, O, N and H, have developed the following (1) an overall scaling factor and (2) a set of 11 factors assigned to different types of molecular deformation defined by nonredundant local symmetry coordinates. They found DFT methods to be reliable for interpretation of infrared spectra and found the scaled B3LYP results superior to the BLYP ones. Next, they derived an additional scale factor of 1.017 for C–Cl stretching coordinates³³ by considering the B3LYP/6-31G* level of theory in a study of isomers of tetrachlorinated dibenzodioxins. This additional scale factor was obtained by fitting the experimental vibrational fundamentals of 1,1-dichloroethene, all four isomers of 1,4-

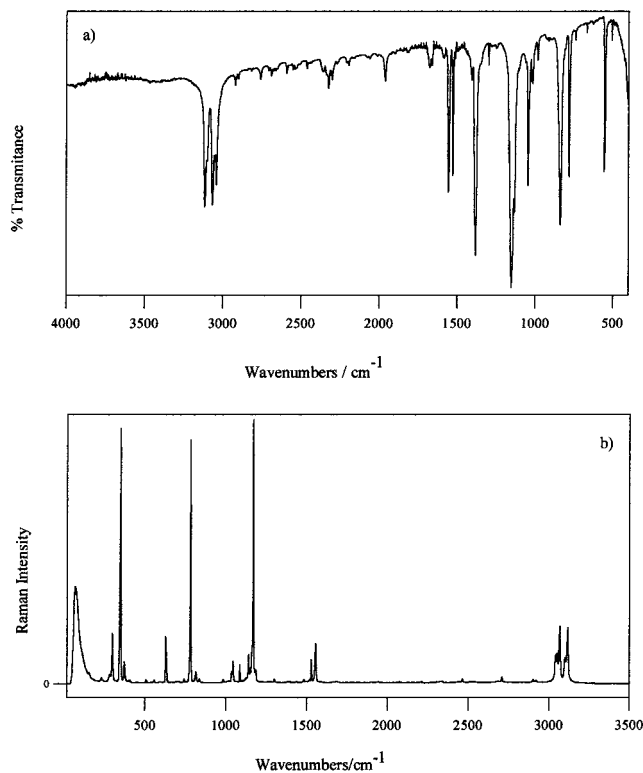


Figure 1. Vibrational spectra of 3,6-dichloropyridazine: (a) IR spectrum in polycrystalline film; (b) Raman spectrum in the solid phase.

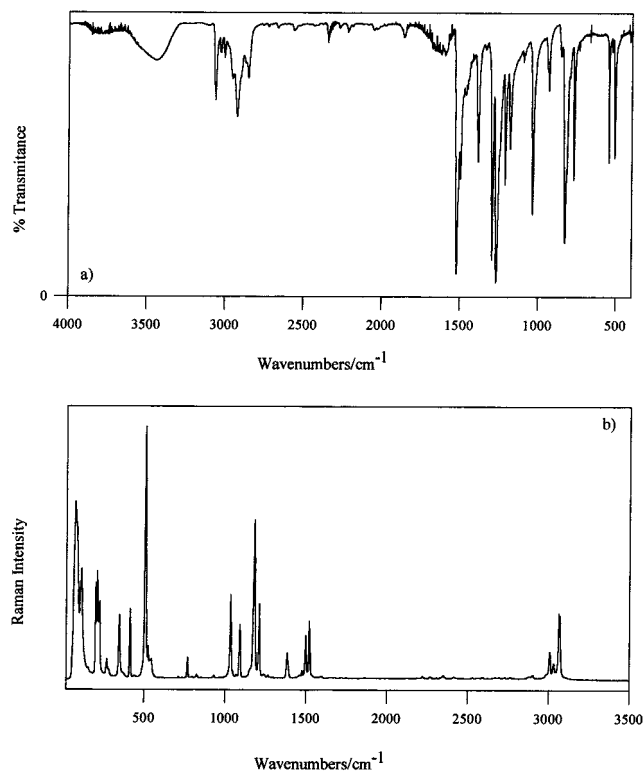


Figure 2. Vibrational spectra of 3,4,5-trichloropyridazine: (a) IR spectrum in KBr disc; (b) Raman spectrum in the solid phase.

dichloro-*trans*-butadiene, chlorobenzene, and *o*- and *m*-dichlorobenzene. More recently, they have presented an alternative approach to the derivation of scaled quantum mechanical (SQM) force fields, scaling the individual primitive force constants from a full set of redundant valence coordinates.³⁴ Again, using the hybrid three-parameter B3LYP density functional with the 6-31G* basis set—the scaling procedure tested for 30 molecules

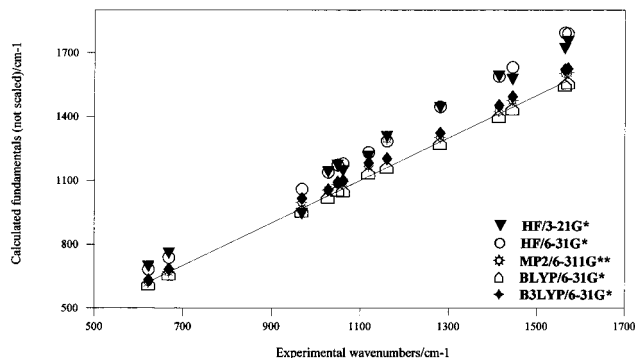


Figure 3. Calculated in-plane vibrational fundamentals of pyridazine using various theoretical methods in comparison with experimental data (line).

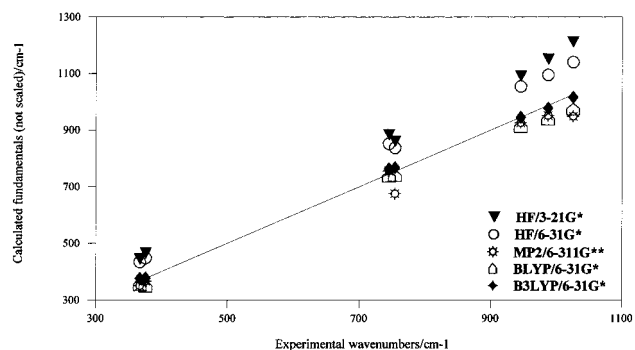


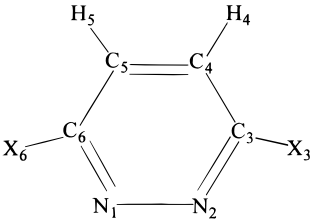
Figure 4. Calculated out-of-plane vibrational fundamentals of pyridazine using various theoretical methods in comparison with experimental data (line).

containing C, O, N, H, and Cl, 24 of which were used in ref 14—gave an average percentage error under 1% in the scaled wavenumbers.

In another approach, Scott and Radom³⁵ compared the computed harmonic vibrational wavenumbers for a set of 122 molecules, using various theoretical methods and basis sets. The methods included HF, second-order Møller–Plesset perturbation theory (MP2), quadratic configuration interaction with singles and doubles substitution (QCISD), and several density functionals, including three hybrid functionals. Global scaling factors for each level of theory were determined by least-squares fit of the calculated to the experimental vibrational wavenumbers. Two of the hybrid density functionals (B3LYP and B3PW91) gave the best overall agreement (after scaling) between theory and experiment.

In addition, there have been many theoretical studies of the vibrational spectrum of pyridazine,^{36–46} several of which developed scaled force fields, obtaining scaled wavenumbers with either a single scale factor⁴¹ or a series of scale factors related to different internal coordinates.^{42,46} In all published cases, the scaling procedure was carried out from quantum mechanical force fields at the HF level. The extensive number of “extra” scale factors applied for certain off-diagonal force constants showed that this is a strongly correlated system where the scaling of HF force fields shows a limited accuracy.

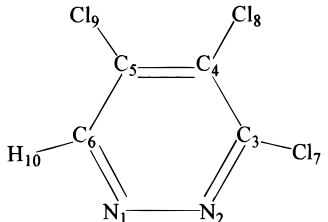
Moreover, it has been proved for many other molecules that DFT methods give computed wavenumbers Figures 3 and 4 with pyridazine as a particular example, and force constants that approximate the experimental ones in a much more systematic fashion than do those from HF theory.⁴⁷ The BLYP/6-31G* wavenumbers are nearer to the experimental ones than are those from B3LYP/6-31G*, although the latter show more uniform deviation from the observed fundamentals, on the order

TABLE 5: Structural Parameters of 3,6-Dichloropyridazine and Pyridazine^a


parameters	3,6-dichloropyridazine						pyridazine						
	ED ^b	ED ^c	HF/ 6-31G**	MP2/ 6-311G** ^c	CCSD/ 6-311G**	BLYP/ 6-31G*	B3LYP/ 6-31G*	a priori ^d	MP2 ^c	CCSD/ 6-311G**	CCSD(T)/ 6-311G**	BLYP/ 6-31G*	B3LYP/ 6-31G*
Bond Lengths/Å													
N ₁ -N ₂	1.339(8)	1.343(3)	1.317	1.344	1.342	1.361	1.339	1.338	1.342	1.336	1.343	1.357	1.336
N ₂ -C ₃	1.334(9)	1.331(3)	1.294	1.333	1.317	1.336	1.322	1.326	1.343	1.332	1.341	1.351	1.336
C ₃ -C ₄	1.373(8)	1.401(3)	1.401	1.402	1.409	1.381	1.404	1.404	1.399	1.403	1.406	1.408	1.399
C ₄ -C ₅	1.377(9)	1.383(3)	1.360	1.384	1.374	1.389	1.378	1.379	1.388	1.382	1.389	1.395	1.384
C ₅ -X ₃	1.717(3)	1.736(3)	1.729	1.725	1.730	1.768	1.747	1.074	1.086	1.086	1.088	1.095	1.087
C ₄ -H ₄	1.109	1.085(13)	1.072	1.084	1.084	1.122	1.084	1.075	1.085	1.085	1.087	1.093	1.086
Angles/Deg													
N ₁ -N ₂ -C ₃	118.6(2)	118.4(2)	119.8	118.9	119.2	118.7	119.1	119.8	119.1	119.3	119.2	119.0	119.4
N ₂ -C ₃ -C ₄	124.6(3)	124.7(4)	123.9	124.6	124.5	124.2	124.5	123.2	124.2	124.0	124.2	124.1	123.8
C ₃ -C ₄ -C ₅	116.8	116.9	116.3	116.5	116.3	117.0	116.4	117.1	116.8	116.7	116.7	116.8	116.8
N ₂ -C ₃ -X ₃	115.4	116.2	116.8	116.1	116.5	116.3	116.2	115.7	114.4	114.8	114.6	114.6	114.9
C ₃ -C ₄ -H ₄	121.0	122.8(13)	123.9	121.2	121.0	121.6	121.2	120.6	120.9	120.9	120.9	120.9	120.9

^a For pyridazine, X = H; for 3,6-dichloropyridazine, X = Cl. ^b Ref 10. ^c Ref 11. ^d Ref 42.

TABLE 6: Structural Parameters of 3,4,5-Trichloropyridazine



parameters	HF/ 3-21G*	HF/ 6-31G*	HF/ 6-31G**	MP2/ 6-311G**	BLYP/ 6-31G*	B3LYP/ 6-31G*
Bond Lengths/Å						
N ₁ -N ₂	1.358	1.309	1.309	1.338	1.353	1.333
N ₂ -C ₃	1.302	1.297	1.297	1.334	1.337	1.324
C ₃ -C ₄	1.405	1.408	1.408	1.412	1.424	1.413
C ₄ -C ₅	1.363	1.368	1.368	1.395	1.403	1.390
C ₅ -C ₆	1.397	1.399	1.398	1.401	1.413	1.403
C ₆ -N ₁	1.308	1.301	1.301	1.335	1.343	1.328
C ₃ -Cl ₇	1.723	1.723	1.723	1.718	1.761	1.739
C ₄ -Cl ₈	1.714	1.713	1.713	1.708	1.744	1.726
C ₅ -Cl ₉	1.720	1.718	1.719	1.715	1.753	1.733
C ₆ -H ₁₀	1.067	1.072	1.073	1.086	1.093	1.086
Angles/Deg						
N ₁ -N ₂ -C ₃	120.2	120.6	120.6	119.6	119.7	120.0
N ₂ -C ₃ -C ₄	123.2	123.4	123.4	124.4	124.3	123.9
C ₃ -C ₄ -C ₅	116.3	115.4	115.4	115.3	115.4	115.4
C ₄ -C ₅ -C ₆	118.2	117.7	117.7	117.6	117.9	117.8
C ₅ -C ₆ -N ₁	122.9	122.8	122.8	123.8	123.4	123.3
C ₆ -N ₁ -N ₂	119.2	120.1	120.1	119.2	119.3	119.6
N ₂ -C ₃ -Cl ₇	116.3	115.7	115.8	115.3	115.4	115.6
C ₃ -C ₄ -Cl ₈	121.6	122.1	122.1	122.7	122.5	122.4
C ₄ -C ₅ -Cl ₉	122.9	123.3	123.3	122.6	122.5	122.7
C ₅ -C ₆ -H ₁₀	119.9	120.4	120.4	120.3	120.5	120.4

of 3%. On the other hand, the inclusion of electron correlation as well as an increase in basis set size to the MP2/6-311G** level improves the values of the calculated wavenumbers obtained from ab initio methods. However, the deviations persist because of anharmonicity, the still-small size of the basis functions,⁴⁸ and the partial treatment of electron correlation.

Bearing in mind the above considerations and results, we resolved to test two different approaches: (1) The B3LYP/6-31G* quantum mechanical force field was taken as a starting point and the optimized scaling factors derived by Pulay et al.¹⁴ were tested to predict the vibrational spectrum of pyridazine, 3,6-dichloropyridazine, and 3,4,5-trichloropyridazine. The scaled a priori spectra constitute *set AI* in Tables 7, 8 and 9 for pyridazine, 3,6-, and 3,4,5-chloropyridazines, respectively. The scale factors from ref 14 were used instead of those from ref 34, because in the former a molecule with an N-N bond (diazirine), similar to the systems in the present study, was included in the training set used to refine the empirical parameters (scale factors). Furthermore, to reduce the differences between experimental and calculated wavenumbers, the scale factors related to C-Cl stretchings and bendings were refined based on observed experimental fundamentals (Tables 1-4). The refined scale factors are shown as *set AII* in Table 10.

(2) To evaluate the particular electronic environment of the pyridazine ring, a set of empirical parameters was refined to correct the B3LYP/6-31G* force field of pyridazine by fitting the calculated to the experimental⁴⁶ wavenumbers. These parameters constitute *set BI* of scale factors (Table 10) which was transferred to 3,6- and 3,4,5-chloropyridazines, obtaining a new a priori vibrational spectrum of each chlorinated molecule. The a priori spectra are defined as *set BI* in Tables 8 and 9 for the di- and trichlorinated derivatives, respectively.

Next, the scale factors related to C-Cl bond displacements, i.e., stretching, bending, and wagging, were refined considering the available experimental evidence of 3,6-dichloropyridazine (Tables 1 and 3). The resulting values are shown in Table 10 as *set BII*. The rest of the scale factors associated with ring and C-H motions were kept fixed (*set BI*). The calculated fundamentals are shown in Table 8 as *set BII*. *set BII* of empirical parameters was transferred to the trichlorinated derivative resulting in the third a priori spectrum of this molecule, which is shown in Table 9 as *set BII*.

Finally, in an effort to reach better agreement between experimental and calculated wavenumbers of 3,4,5-trichloro-

TABLE 7: Experimental and Scaled Wavenumbers (cm^{-1}) and Character of the Vibrations of Pyridazine from B3LYP/6-31G* Calculations

	exps ^{a,b}	scals ^c		description
		set A1	set B1	
A ₁ Symmetry				
ν_1	3086	3087.1	3089.2	C–H str.
ν_2	3071	3063.9	3065.8	C–H str.
ν_3	1570	1570.3	1566.6	ring str., C–H def.
ν_4	1444	1448.1	1440.4	ring str., C–H def.
ν_5	1160	1156.9	1158.0	ring str.
ν_6	1119	1147.3	1140.3	C–H def., N–N str.
ν_7	1061	1060.3	1059.5	C–H def., ring str.
ν_8	968	968.0	977.0	ring str.
ν_9	665	676.4	666.1	ring def.
A ₂ Symmetry				
ν_{10}	1025 ^d	1008.6	1015.4	C–H wag.
ν_{11}	945	935.6	943.4	C–H wag.
ν_{12}	754	739.4	753.6	torsion
ν_{13}	367	363.1	369.8	torsion
B ₁ Symmetry				
ν_{14}	987	968.5	975.9	C–H wag.
ν_{15}	745	756.1	762.6	C–H wag.
ν_{16}	376	364.3	371.2	torsion
B ₂ Symmetry				
ν_{17}	3079	3075.1	3077.1	C–H str.
ν_{18}	3057	3059.0	3060.9	C–H str.
ν_{19}	1563	1565.9	1561.9	ring str., C–H def.
ν_{20}	1413	1409.6	1401.2	C–H def., C–N str.
ν_{21}	1281	1283.1	1276.6	C–H def., C–N str.
ν_{22}	1049	1060.7	1053.1	ring str., C–H def.
ν_{23}	1027 ^d	1041.4	1029.7	ring def.
ν_{24}	622	627.6	617.6	ring def.

^a Ref 46. ^b Experimental wavenumbers were selected from the gas-phase spectra; when they were not available, data from liquid and solid phases were used. ^c For *set A1* and *set B1*, see text. ^d Both fundamentals show close wavenumbers; see ref 46.

pyridazine, as well as to prove the whole idea of the scaling procedure which assumes that every single molecule does not need an individual scaling to be correctly analyzed in its vibrational spectrum, the scale factors related to ring stretchings and C–H bendings were refined (*set BIII*, Table 10) by considering the experimental information (Tables 2 and 4) for this molecule. The calculated fundamentals are shown in Table 9 defining the *set BIII*.

To carry out all these steps, the output of Cartesian force constants together with the corresponding Cartesian coordinates for each atom were fed into the program ASYM40 (an update of ASYM20),⁴⁹ and the force constants were transformed into nonredundant local symmetry coordinates⁵⁰ considering the internal coordinate definitions shown in Figure 5. The theoretical geometry was used without any empirical correction. The B3LYP/6-31G* force constants were scaled according to Pulay's method,⁵⁰ using the program SCALE3⁵¹ for the *Series A* of scalings and the program ASYM40 for the *Series B*. Both programs permit refinement of scale factors associated with each diagonal symmetry force constant by least-squares fitting to every kind of vibrational datum that stems from the force field. The program ASYM40 was also used to calculate the **B** matrix and to obtain the potential energy distribution (PED) in the normal coordinate system.

IV. Discussion and Results

IV. 1. Structure. We have determined the structural parameters of 3,6-dichloropyridazine in its ground state at the HF/3-21G*, HF/6-31G*, HF/6-31G**, MP2/6-311G**, CCSD/6-

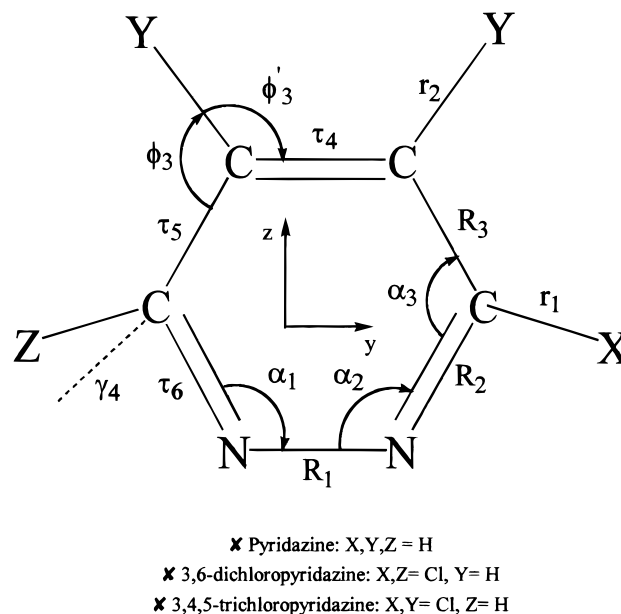


Figure 5. Valence internal coordinates in pyridazines series. γ is the wagging coordinate and τ is Wilson, ring torsion.⁵⁹ (around the bond indicated), defined as in ref 49. In the wagging coordinates, the H atoms move in the positive X direction.

311G**, BLYP/6-31G*, and B3LYP/6-31G* levels. Recently Morrison et al.¹¹ published the theoretical equilibrium geometries of 3,6-dichloropyridazine at the HF/3-21G*, HF/6-31G*, MP2/6-31G*, and MP2/6-311G** levels. Accordingly, in Table 5 only the newly calculated theoretical data are presented. The equilibrium geometry of 3,6-dichloropyridazine determined at the MP2/6-311G** level by Morrison et al.¹¹ (showing only marginal differences from our calculated data) are repeated in the table for better comparison. Experimental data originating from the papers of Almenningen et al.¹⁰ and Morrison et al.¹¹ are also presented in Table 5. Since the chloro-substituted pyridazines are closely related to the pyridazine molecule itself, the earlier empirically corrected HF/4-21G theoretical geometry,⁴² so-called "a priori" geometry, as well as the theoretical MP2/6-311G** geometry of Morrison et al.¹¹ of pyridazine are also shown in Table 5. We decided to repeat the calculations of the equilibrium structure of pyridazine with the high-level electron correlation methods CCSD and CCSD(T): in these calculations we used the 6-311G** basis set for better comparison with the theoretical results on 3,6-dichloropyridazine. These new results are also presented in Table 5. The crystal structures of pyridazine⁵² and 3,6-dichloropyridazine¹¹ are not shown here because they correspond to the solid state.

With the tested quantum mechanical methods, the worst calculated angles show differences on the order of 2° with respect to the experimental information.¹⁰ The more accurate ab initio methods, MP2/6-311G** and CCSD/6-311G**, differ from experiment by less than 0.5° in all cases, and DFT is not far behind.

By contrast, larger discrepancies with the electron diffraction data¹⁰ were observed in the bond lengths. In particular, Figure 6 displays the absolute values of the ring bond lengths of 3,6-dichloropyridazine from MP2/6-31G**, CCSD/6-311G**, BLYP/6-31G*, and B3LYP/6-31G* theoretical methods other than those experimentally obtained from ref 10.

The geometric parameters of 3,6-dichloropyridazine were successfully converged with systematic improvements of basis set size and treatment of electron correlation.¹¹ The increase in the basis set size at the HF level does not significantly improve

TABLE 8: Experimental and Scaled Wavenumbers (cm⁻¹), Theoretical IR Intensities (km²mol⁻¹), and Character of the Vibrations of 3,6-Dichloropyridazine from B3LYP/6-31G* Calculations

	exps ^a		calc IR intensity	scals ^b				description
	IR	Raman		set AI	set AII	set BI	set BII	
A ₁ Symmetry								
ν_1	3091 ^c	3091 ^c p	0.09	3111.0	3111.1	3113.2	3113.2	C-H str.
ν_2	1556 s	1556 w dp	7.75	1550.9	1551.0	1548.3	1548.4	ring str.; C-H def.
ν_3	1299 w	1299 s p	1.55	1287.4	1292.0	1285.0	1291.1	ring str.
ν_4	1168 s	1164 s p	0.25	1155.9	1155.3	1156.9	1156.6	ring str.
ν_5	1147 vs	1141 s p	4.59	1139.3	1143.8	1134.8	1140.9	ring str.; C-H def.
ν_6	1045 s	1044 vvs p	5.59	1044.5	1054.4	1044.4	1056.6	ring str.
ν_7	780 s	781 vvs p	7.26	776.9	784.4	771.2	781.4	C-Cl str.; ring def.
ν_8	343 vvw	349 vvs p	0.02	334.5	342.9	332.4	342.7	ring def.; C-Cl str.
ν_9		232 vvw	0.11	224.5	231.0	218.7	227.6	C-Cl def.
A ₂ Symmetry								
ν_{10}	983 w	984 w		983.6	983.6	990.7	990.6	C-H wag.
ν_{11}	741 vvw	742 w		725.0	725.0	737.1	735.7	torsion; C-Cl wag.
ν_{12}	407 vw	407 vw		400.0	400.0	406.8	406.2	torsion; C-Cl wag.
ν_{13}	298 vw	299 s dp		289.7	289.7	293.4	291.6	C-Cl wag.; torsion
B ₁ Symmetry								
ν_{14}	836 s	836 w	27.16	839.3	839.3	846.5	845.6	C-H wag.
ν_{15}	507 w	508 w dp	0.28	503.4	503.4	508.8	505.5	C-Cl wag.; torsion
ν_{16}		114/156 sh/w	0.03	90.8	90.8	92.2	92.1	torsion
B ₂ Symmetry								
ν_{17}	3074 ^c	3074 ^c dp	0.24	3098.7	3098.7	3100.7	3100.7	C-H str.
ν_{18}	1528 s	1528 m dp	4.26	1522.6	1524.2	1520.8	1522.8	ring str.
ν_{19}	1387 vvs	1387 vw, br dp	207.08	1378.9	1379.9	1373.5	1374.9	ring str.; ring def.
ν_{20}	1129 vvs	1126 w p?	258.74	1124.2	1133.8	1116.2	1128.6	ring str.; C-H def.
ν_{21}	1019 m	1017 w	10.12	1018.4	1018.9	1009.5	1010.7	ring def.; ring str.
ν_{22}	628 m	628 s dp	2.00	629.1	630.9	618.9	621.3	ring def.
ν_{23}	555 s	557 w dp	41.19	524.9	545.0	523.6	548.9	C-Cl str.
ν_{24}	372 vw, br	373 w dp	2.70	373.9	384.5	363.7	378.3	C-Cl def.

^a Abbreviations: s, strong; m, medium; w, weak; v, very; br, broad; sh, shoulder; p, polarized; dp, depolarized. ^b Sets A and B, see text. ^c Unperturbed wavenumbers calculated considering a Fermi resonance, see text.

TABLE 9: Experimental and Scaled Wavenumbers (cm⁻¹), Theoretical IR Intensities (km²mol⁻¹), and Character of the Vibrations of 3,4,5-Trichloropyridazine from B3LYP/6-31G* Calculations

	exps ^a		calc IR intensity	scals ^b					description
	IR	Raman		set AI	set AII	set BI	set BII	set BIII	
A' Symmetry									
ν_1	3069 s	3070 s p	0.81	3091.7	3091.7	3093.7	3093.8	3093.8	C-H str.
ν_2	1519 vs	1520 s dp	93.88	1502.6	1504.7	1499.8	1502.6	1513.8	ring str.; C-H def.
ν_3	1498 vs	1499 s dp	22.31	1483.9	1485.6	1482.6	1484.7	1491.5	ring str.
ν_4	1382 s	1384 m dp	15.23	1372.4	1376.1	1367.5	1372.5	1387.7	ring str.; C-Cl str.; C-H def.
ν_5	1267 vs	1265 w dp	183.67	1262.0	1270.0	1260.2	1270.9	1275.3	ring str.; C-Cl str.; C-Cl def.
ν_6	1210 vs	1212 s p	17.68	1187.6	1198.6	1184.5	1198.9	1208.9	ring str.; C-H def; C-Cl str.
ν_7	1179 m	1180 vs p	14.98	1166.9	1167.5	1168.6	1169.0	1175.3	ring str.
ν_8	1095 vw	1093 s p	9.37	1078.9	1089.9	1071.5	1085.5	1087.8	ring str.; ring def.; C-Cl str.
ν_9	1034 vs	1035 s p	33.86	1041.1	1047.7	1036.6	1046.1	1048.6	ring def.; ring str.; C-Cl str.
ν_{10}	826 vs	826 w	105.36	808.9	827.7	802.9	828.8	828.3	C-Cl str.; ring def.
ν_{11}	770 vs	770 m dp	11.47	753.9	766.0	746.4	761.7	762.0	ring def.; C-Cl str.
ν_{12}	509 s	507 vs p	13.14	498.4	510.3	490.6	507.9	508.3	C-Cl str.; C-Cl def.; ring str.
ν_{13}	485 br, sh		2.75	486.4	501.5	484.0	501.4	501.8	C-Cl str.; ring str.
ν_{14}	413 w	414 s dp	1.05	406.2	417.3	399.8	414.5	414.8	C-Cl def.; ring str.
ν_{15}	344 vw	348 s p?	0.24	336.2	344.1	333.4	343.1	343.1	ring def.; C-H str.
ν_{16}	223 w	217 s dp	0.05	206.2	212.0	201.0	208.9	209.0	C-Cl def.
ν_{17}		211 s dp	0.04	199.8	205.7	194.5	202.6	202.6	C-Cl def.
A'' Symmetry									
ν_{18}	931 m	932 vw	6.57	915.1	915.1	922.1	921.8	921.8	C-H wag.
ν_{19}	738 vw	738 vw vw	0.00	723.0	723.0	734.0	731.8	731.8	torsion; C-Cl wag.
ν_{20}	547 s	546 w p	5.84	548.7	548.7	555.5	552.0	552.0	C-Cl wag.; torsion
ν_{21}	526 w	526 m p	0.23	528.2	528.2	534.3	530.6	530.6	C-Cl wag.; torsion
ν_{22}	269 w	271 m m p	1.25	256.3	256.3	258.7	256.5	256.5	C-Cl wag.
ν_{23}		202 s dp	6.03	196.1	196.1	199.2	198.9	198.9	torsion; C-H wag.
ν_{24}		112/81 s/sh dp	0.06	75.1	75.1	76.3	76.3	76.2	torsion

^a Abbreviations: s, strong; m, medium; w, weak; v, very; br, broad; sh, shoulder; p, polarized; dp, depolarized. ^b Sets A and B, see text.

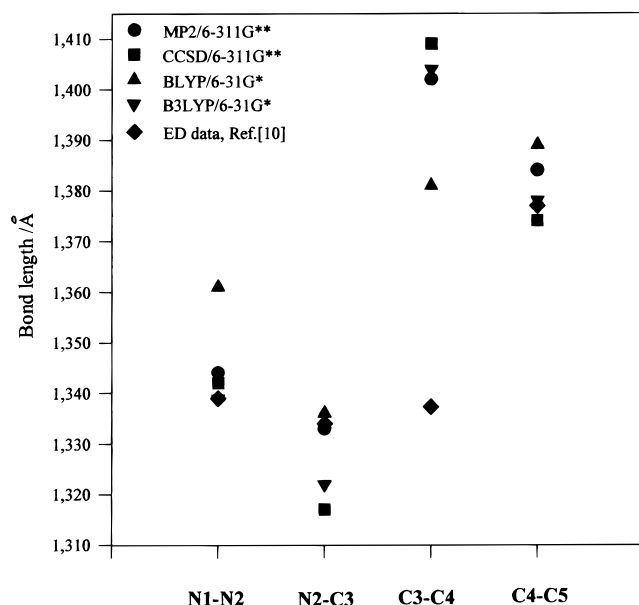
the bond lengths. Addition of *p* functions on hydrogens changed the value of the C₃-C₄-H₄ valence angle only. The inclusion of some part of the electron correlation effects improved the

theoretical values (see Figure 6 and Table 5). It can be observed that the HF level yields shorter bond lengths, especially for the N₁-N₂, N₂-C₃, and C₄-C₅ bonds, and the MP2 method

TABLE 10: Scaling Factors for the Different Types of Internal Coordinates

coordinates	scaling factors ^a				
	set AI	set AII	set BI	set BII	set BIII
	In-Plane				
ring stretching	0.922	0.922	0.925	0.925	0.933 ^d
C–H stretching	0.920	0.920	0.921	0.921	0.921
C–Cl stretching	0.922	1.013 ^b	0.921	1.039 ^c	1.039
ring def.	0.990	0.990	0.956	0.956	0.956
C–H def.	0.950	0.950	0.933	0.933	0.979 ^d
C–Cl def.	0.990	1.055 ^b	0.933	1.020 ^c	1.020
	Out-of-Plane				
C–H wagging	0.976	0.976	0.993	0.993	0.993
C–Cl wagging	0.976	0.976	0.993	0.974 ^c	0.974
torsion	0.935	0.935	0.968	0.968	0.968

^a Sets A, optimized scaling factors derived from a training set of 30 molecules, ref 14; sets B, optimized scaling factors defined for pyridazines series. See text. ^b Refined scaling factors derived from the experimental wavenumbers of both chloropyridazines. ^c Refined scaling factors obtained from the experimental wavenumbers of 3,6-dichloropyridazine. ^d Refined scaling factors derived from the experimental wavenumbers of 3,4,5-trichloropyridazine.

**Figure 6.** Ring bond distances of 3,6-dichloropyridazine from various theoretical and experimental methods.

somewhat overestimates them (Figure 6). The values determined at the CCSD level are between the values of the two aforementioned levels but closer to the MP2 ones. We have not determined the equilibrium structure of 3,6-dichloropyridazine at the CCSD(T) level due to the much larger requirement for computer time. In particular, the bond lengths calculated at the BLYP/6-31G* level are systematically overestimated,⁵³ especially for the C₃–Cl₃ bond (see Table 5). The B3LYP method gave distances and angles nearer to the theoretical values at the CCSD level.

One previous study of Bérces et al.⁴² dealt with the a priori molecular structure and SQM force field of pyridazine. They considered their a priori molecular structure as the best equilibrium geometry for gaseous pyridazine. Those results⁴² showed less aromatic character for pyridazine than usually expected: this fact was manifested by the small but significant alternation of the bond lengths around the ring (cf. Table 5). Their conclusion was in accordance with the results of both simple Hückel molecular orbital method and the π -electron version of the valence bond theory (see ref 42 and references

therein). Using this model of the electron structure of pyridazine, i.e., a shift from the heteroaromatic character toward one of the Kekulé structures, they criticized the results of Cradock et al.,⁵⁴ who obtained their final molecular structure by combining their own electron diffraction (ED) and LC NMR data⁵⁴ with the microwave (MW) data of Werner et al.⁵⁵ Very likely, the MW data of Werner et al.⁵⁵ have serious insufficiencies due to the fact that two of the carbon atoms are very close to one of the principal axes of inertia; thus Cradock et al.⁵⁴ did not get any alternation in the pyridazine ring. The present CCSD and CCSD(T) calculations, even with very small computed differences between the N–N and C–N bonds, mark a fine preference for one of the Kekulé structures.

Thus, we consider the Kekulé-type character as the most important feature of the pyridazine ring for both the pyridazine and 3,6-dichloropyridazine molecules. This fact was also independently shown for both molecules by X-ray diffraction.^{11,52} Moreover, our conclusion agrees with the results of Wiberg et al.,⁵⁶ who have also found a smaller resonance energy via systematic calculation of the hydrogenation energy for pyridazine.

Accordingly, the ED results of Almenningen et al.¹⁰ should not be considered appropriate for the 3,6-dichloropyridazine (see Figure 6): the alternation fails for the ring bond lengths, obviously, in the case of the C₃–C₄ and C₄–C₅ bonds. The torsion in this ring structure¹⁰ was very likely initiated because the authors introduced the essentially erroneous MW data of Werner et al.⁵⁵ as constraints into the ED structure refinement. From this point of view of the alternation for the ring bond lengths, the results obtained at the BLYP/6-31G* level could not be accepted as an adequate structure for the ring, either.

The gas electron diffraction (GED) structure of Morrison et al.¹¹ is essentially correct for 3,6-dichloropyridazine, considering the undoubted alternation around the ring. On the other hand, we think that the GED value for the N₁–N₂ bond length of Morrison et al.¹¹ could be somewhat overestimated, because their values¹¹ were derived by the combination of experimental and theoretical data via the SARACEN method.⁵⁷ Obviously, their final values are strongly influenced by their ab initio geometric parameter restraints, which were obtained at the MP2/6-311G** level. In fact, especially for bonds between electronegative elements, calculations performed at the MP2 level practically always produce greater values for equilibrium bond lengths than the corresponding experimental data because of the improper description of the antibonding orbitals in the wave function.^{16,58} Also, one can observe an unbalanced value of the N₂–C₃ bond length in case of their pyridazine calculation¹¹ (see Table 5): the alternation breaks for the case of the N₁–N₂ and N₂–C₃ bonds, respectively. This means that even the N₂–C₃ bond length is slightly overestimated at the MP2/6-311G** level. Transferring this conclusion for the case of 3,6-dichloropyridazine, we can estimate a somewhat larger $r(\text{N–N}) - r(\text{C–N})$ bond length deviation than was considered in paper of Morrison et al.¹¹ Obviously, this argument affects the observed GED data of Morrison et al.¹¹ because of the SARACEN method.⁵⁶ Here the basic agreement between the a priori molecular structure for pyridazine⁴² and the present CCSD and B3LYP data of 3,6-dichloropyridazine should be emphasized. There is also a disagreement between the ring parameter values of Morrison et al.¹¹ corresponding to pyridazine and 3,6-dichloropyridazine at the MP2/6-311G** level.

Summing up, the Kekule alternation is present in all the results except BLYP (Figure 6). In particular, about the ring

bonds, the CCSD and B3LYP methods give the same picture; however, for the C–Cl bond, CCSD seems better.

To our knowledge, there is not an experimental structure for 3,4,5-trichloropyridazine in the literature. We publish our theoretical equilibrium structure calculated at different HF, MP2, and DFT levels in Table 6. All theoretical methods suggest C_s symmetry for 3,4,5-trichloropyridazine.

One can observe similar trends comparing the different theoretical structures to each other for 3,4,5-trichloropyridazine (see Table 6) as for 3,6-dichloropyridazine in Table 5 (e.g., the bond lengths computed at the BLYP levels are overestimated compared to those at the B3LYP level). Because of the similar electron configurations of 3,6-dichloropyridazine and 3,4,5-trichloropyridazine, it is reasonable to assume similar trends for the quality of the theoretical levels investigated. In this context we consider the ring of 3,4,5-trichloropyridazine to be also less aromatic than other common azines and diazines. The equilibrium structure calculated at the B3LYP/6-31G* level would be the most appropriate to describe this condition. One can observe a small overestimation for the values of the N_2 – C_3 and C_6 – N_1 bond lengths at the MP2/6-311G** level in comparison with those at the B3LYP level.

IV. 2. Analysis of the Scaling Procedures. Pyridazine. To fit the calculated wavenumbers of pyridazine to the experimental data,⁴⁶ only six scale factors were defined in each of the two scaling procedures tested (*set AI* and *set BI*, Table 10). Their values were of the order of 0.9–1.0. Although the scale factors related to the stretching coordinates showed similar values in *set AI* and *set BI*, larger differences were observed for the rest of the scaling parameters, with the largest deviations in the ring deformation and torsion scale factors. This could be due to the particularly low aromaticity of the pyridazine ring, which could not be correctly evaluated from the *set AI* of scale factors obtained from a training set where only rings of benzene and pyridine were chosen. The latter present a significantly larger aromatic character than for pyridazine. However, *set AI* gives reasonable rms values of 9.3 and 12.9 cm^{-1} for in-plane and out-of-plane vibrations, respectively [where rms denotes the root-mean-square deviation defined in footnote (a) of Table 11]. The maximum deviation was 28.3 cm^{-1} for the ν_6 fundamental. When the experimental spectrum of pyridazine was considered, the rms values became only 6.9 and 8.8 cm^{-1} for in-plane and out-of-plane vibrations, respectively (Table 7), with a maximum deviation of 21.3 cm^{-1} persisting for ν_6 . The ν_{10} normal mode was not considered as an observed data point in the scaling because it is still subject to significant experimental uncertainty. Thus, the scaled wavenumbers of this mode constitute a prediction.

It is interesting to underline the importance of the initial quantum mechanical force field used in the scaling procedure. For instance, the B3LYP/6-31G* scaled quantum mechanical force field made it possible to reach a different decision than previous studies which left doubts about the assignment of the torsional mode ν_{12} between two Raman depolarized bands at 729 cm^{-1} and at 754 cm^{-1} . Although the former was selected by the HF scaled force fields,⁴⁶ for the DFT force field the latter is nearer to the scaled wavenumber.

3,6-Dichloropyridazine. The six scale factors calibrated from pyridazine (*set BI*) as well as those derived from a training set of 30 molecules¹⁴ (*set AI*) were transferred to 3,6-dichloropyridazine. The a priori calculated spectra were decisive enough to enable us to propose a vibrational assignment from the experimental evidence for this molecule. The resulting scaled wavenumbers are shown in Table 8 (*sets AI* and *BI*). The rms

TABLE 11: Root Mean Square Deviations (cm^{-1}) of the Calculated Fundamentals of Pyridazine Series from Different Scaling Procedures^a

vibrations	<i>set AI</i>	<i>set AII</i>	<i>set BI</i>	<i>set BII</i>	<i>set BIII</i>
Pyridazine					
in-plane	9.3	9.3	6.9		
out-of-plane	12.9	12.9	8.8		
total	10.7	10.7	7.5		
3,6-Dichloropyridazine					
in-plane ^b	10.5	6.5	12.2	6.5	
out-of-plane ^c	11.8	11.8	6.0	6.1	
total	11.1	8.2	10.8	6.4	
3,4,5-Trichloropyridazine					
in-plane ^b	12.9	9.1	16.0	9.7	7.7
out-of-plane ^c	10.6	10.6	8.3	6.4	6.4
total	11.7	9.5	14.3	8.9	7.4

^a See text and Table 10 for definition of the scaling procedures. The root mean square deviations (rms) of the calculated fundamentals from the various scaling procedures were defined by

$$\text{rms} = \sqrt{\frac{\sum_i (\omega_i^{\text{theor}} - \nu_i^{\text{expt}})^2}{N}}$$

where ω_i^{theor} and ν_i^{expt} are the i^{th} theoretical harmonic and i^{th} experimental fundamental wavenumbers (in cm^{-1}), respectively, and N denotes the number of modes. ^b The CH stretching fundamentals were not considered. ^c The lowest fundamental was not considered. See text.

values for with respect to the selected in-plane fundamentals were 10.5 and 12.2 cm^{-1} (C–H stretchings not considered) for *sets AI* and *BI*, respectively, and 10.8 and 6.0 cm^{-1} for out-of-plane modes for *sets AI* and *BI*, respectively. In both sets, the largest deviation found was for ν_{23} , calculated at 32.1 cm^{-1} (*set AI*) and 30.4 cm^{-1} (*set BI*) smaller than the experimental value.

When the scale factors related to C–Cl displacements were refined by considering the experimental wavenumbers of this molecule, the rms values were reduced. C–Cl stretching and bending scale factors were fitted to give the parameters of *set AII* scale factors, which reduced the rms for in-plane vibrations to 6.5 cm^{-1} . In *set BI* the scale factors related to C–Cl stretching, bending, and wagging were also refined; they constitute *set BII*. Although the rms values for out-of-plane modes were not significantly improved, the in-plane rms was reduced to 6.5 cm^{-1} (Table 11). The maximum deviation amounted to 12.1 cm^{-1} for the B_2 symmetry mode, ν_{19} .

It can be observed in Table 10 that the scale factors associated with C–Cl stretching and bending internal coordinates show large values: 1.013 and 1.055, respectively, in *set AII* and 1.039 and 1.020, respectively, in *set BII*. Also, Pulay et al. in their different studies^{33,34} obtained values between 1.0438 and 1.017 for the C–Cl stretching scale factor using the same level of theory for the initial quantum mechanical force field. The high value of these scale factors can be due to the overestimation of the C–Cl bond distance calculated with the B3LYP/6-31G* method, 0.03 Å larger than the experimental value. As a consequence of the large bond length, the C–Cl stretching force constant is underestimated, requiring a scale factor larger than 1.0. With respect to the C–Cl bending scale factor, it is difficult to explain its value considering the C–Cl bond distance. Qualitatively the situation could be interpreted by taking into account that an overestimated C–Cl bond distance reduces the interaction between the electron density of the chlorine atom and the lone-pair electrons of the nitrogen atoms in the ring, leading to an underestimation of the related force constants.

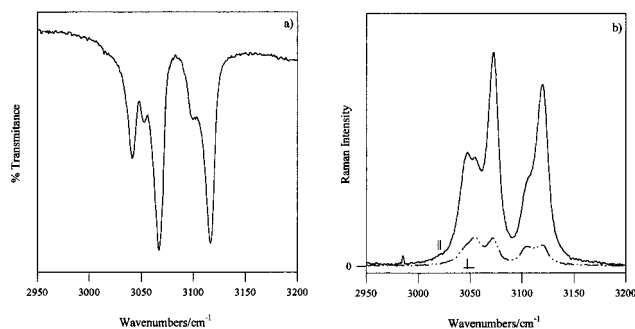


Figure 7. Vibrational spectrum of 3,6-dichloropyridazine in the region of 2950–3200 cm^{-1} : (a) IR spectrum (b) Raman spectrum, parallel (||) and perpendicular (\perp), in CCl_4 solution.

3,4,5-Trichloropyridazine. The scale factors of *sets AI* and *BI* were transferred to trichloropyridazine, and the resulting scaled wavenumbers, shown in Table 9, represent the first a priori spectra of this molecule. The calculated fundamentals were used to define a first assignment of the vibrational spectrum. The experimental wavenumbers selected as fundamentals show rms deviations of 12.9 and 16.0 cm^{-1} for in-plane modes with *sets AI* and *BI*, respectively, and 10.6 and 8.3 cm^{-1} for out-of-plane vibrations with *sets AI* and *BI*. Both sets present a maximum deviation on the order of 23 cm^{-1} for the ν_6 normal mode. As with 3,6-dichloropyridazine, the normal modes corresponding to the C–Cl displacements present the largest discrepancies.

Subsequently, a priori spectra using the scale factors defined for 3,6-dichloropyridazine and including factors for the C–Cl motions were used. These are shown in Table 9 as *sets AII* and *BII*. In these cases the rms values amounted to 9.1 and 9.7 cm^{-1} for in-plane vibrations (C–H stretching not included) with *sets AII* and *BII*, respectively, and 10.6 and 6.4 cm^{-1} for out-of-plane modes with *sets AII* and *BII*. With *set AII* the largest deviation was 16.5 cm^{-1} for ν_{13} and with *set BII* it was 17.3 cm^{-1} for the ν_2 normal mode. Finally, to determine whether check if a better agreement between calculated and experimental wavenumbers could be reached, the scale factors related to ring stretching and C–H bending internal coordinates were refined by considering as reference the experimental evidence of this trichlorinated derivative with the result shown in Table 9 as *set BIII*. It is observed that the rms deviations were not significantly improved, showing values of 7.7 cm^{-1} for in-plane vibrations (C–H stretching not included) with maximum deviations on the order of 16.8 cm^{-1} . These results prove that further specific scale factors for each individual molecule are not necessary.

It can be concluded that *sets AI* and *BI* are equally effective in predicting a priori spectra of these two molecules. However, *set BII* turns out to be more useful than *set AII* to refine the vibrational assignments, especially for the normal modes related to out-of-plane vibrations and C–Cl displacements located in the most confused spectral ranges. Insignificant differences were found when a special scaling procedure for 3,4,5-trichloropyridazine was developed (*set BIII*).

IV. 3. Assignment. 3,6-Dichloropyridazine. A_1 Symmetry. The highest A_1 symmetry fundamental, ν_1 , could be assigned to either of the two Raman polarized bands at 3116 or 3067 cm^{-1} . However, based on the relative intensities of these bands in the infrared and Raman spectra (Figure 7a,b), as well as examination of this spectral region in the pyridazine spectrum,⁴⁶ we propose a Fermi resonance^{59,60} between these two A_1 bands. An approximate quantitative correction to the resonance was carried out by applying the intensities method.⁶¹ The unperturbed bands were calculated to be at 3093 and 3091 cm^{-1} . One of

the unperturbed bands was assigned to the C–H stretching normal mode, ν_1 , and the other one to the first overtone of ν_2 , i.e., $2\nu_2$.

The next A_1 symmetry fundamental was assigned to the infrared and Raman bands at 1556 cm^{-1} (Table 8). Although this band does not appear polarized in Raman, the assignment was supported by taking into account the same behavior observed for this ring-stretching mode in pyridazine,⁴⁶ as well as by the calculated values from the scaled quantum mechanical force field and the qualitative results for the IR intensities reported by the B3LYP/6-31G* method (Table 8).

The rest of the A_1 normal modes were assigned by considering the relative, experimental, and calculated intensities of the bands, the Raman polarization behavior and the results of the quantum mechanical force field (Table 8). Thus, ν_3 , ν_4 , ν_5 , ν_6 , ν_7 , and ν_8 were identified with the infrared bands at 1299, 1168, 1147, 1045, 780, and 343 cm^{-1} and to the Raman bands at 1299, 1164, 1141, 1044, 781, and 349 cm^{-1} , respectively. As seen in Table 8, the description of some normal modes appears mixed. Fundamentals such as ν_4 , ν_5 , and ν_6 , traditionally related with pure ring stretchings, now show small contributions of C–H bendings and C–Cl bendings and stretchings. However, ν_7 , assigned at 780 cm^{-1} (IR), represents a more pure C–Cl symmetric stretching, although a C–Cl stretching contribution is also present in ν_8 at 343 cm^{-1} in IR and at 349 cm^{-1} in Raman.

The vibration of A_1 symmetry with the lowest wavenumber, ν_9 , was related to the weak band in the Raman spectrum at 232 cm^{-1} , whose polarization ratio could not be determined. However, the calculations predict a wavenumber for this C–Cl bending mode near this experimental band. This assignment agrees with those found for the C–Cl bending mode in 4,6-dichloropyrimidine at 210 cm^{-1} ^{8a} and in 2,6-dichloropyridazine at 183 cm^{-1} .⁹

B_2 Symmetry. As was the case for ν_1 , the highest B_2 symmetry fundamental could be assigned to either of the Raman depolarized bands at 3100 or 3052 cm^{-1} . Nevertheless, taking into account their very similar relative intensities (Figure 7a,b), a Fermi resonance of B_2 symmetry is proposed. The intensities method⁶¹ was again applied to estimate the unperturbed wavenumbers as 3076 and 3074 cm^{-1} . One of them was identified with ν_{17} and the other was assigned to a combination band, i.e., $\nu_2 (A_1) + \nu_{18} (B_2)$, as a possible option.

Those bands that showed the highest intensity, showed a depolarization ratio in line with the B_2 symmetry, and were in agreement with the scaled wavenumbers and the predicted IR intensities were assigned to the remaining B_2 modes. Thus, ν_{18} , ν_{19} , ν_{20} , ν_{21} , ν_{22} , ν_{23} , and ν_{24} were related to the IR bands at 1528, 1387, 1129, 1019, 628, 555, and 372 cm^{-1} and to the Raman bands at 1528, 1387, 1126, 1017, 628, 557, and 373 cm^{-1} , respectively. The weakness of the Raman bands of ν_{20} and ν_{21} made it impossible to evaluate their depolarization ratios. From the quantum mechanical force field, the description of some normal modes appears mixed. The typical ring modes, as with the A_1 fundamentals, showed contributions of C–H bendings and C–Cl bendings and stretchings. However, ν_{22} at 628 cm^{-1} in the IR and Raman spectra, represented a pure asymmetric ring bending. Also, ν_{23} at 555 cm^{-1} could be assigned to a pure asymmetric C–Cl stretching (Table 8). The latter assignment agrees with those found for this mode in *p*-dichlorobenzene⁶² and in 4,6-dichloropyrimidine,^{8a} where it was identified at 545 and 445 cm^{-1} , respectively. However, in 2,6-dichloropyridazine⁹ this mode was assigned to a higher wavenumber band at 828 cm^{-1} .

Finally, the asymmetric C–Cl bending, ν_{24} , was assigned as the bands at 373 and 372 cm^{-1} in the Raman and IR spectra, respectively. Comparing with other chlorinated aromatic cyclic molecules, the same mode was assigned at 395 cm^{-1} in 4,6-dichloropyrimidine,^{8a} at 332 cm^{-1} in 2,6-dichloropyrazine,⁹ and in the same spectral region in *p*-dichlorobenzene.⁶²

A₂ Symmetry. For a molecule with C_{2v} symmetry, the selection rules require that A_2 symmetry fundamentals be inactive in the infrared. However, no bands were found that were present only in the Raman spectrum that could be assigned to A_2 modes. Breaking of the selection rules is caused by intermolecular interactions, particularly strong in the solid phase, which cause a distortion of the C_{2v} molecular symmetry. It should be considered that this symmetry point group was obtained from an electron diffraction experiment¹⁰ where the molecule is in the gas phase, and from quantum mechanical calculations where the molecular system is considered isolated. In fact, Morrison et al.¹¹ also reported the crystal structure of this dichlorinated compound and identified the distortions that occur on crystallization due to the intermolecular bonding $N\cdots H$ interactions between neighboring molecules. Thus, we have assigned the C–H wagging mode, ν_{10} , to the IR band at 983 cm^{-1} and the Raman band at 984 cm^{-1} . The torsion modes, ν_{11} , ν_{12} , and ν_{13} , were associated to the bands at 741, 407, and 298 cm^{-1} and at 742, 407, and 299 cm^{-1} in the IR and Raman spectra, respectively. The Raman bands did not show a significant intensity except the one at 299 cm^{-1} , which also was observed in the IR with Nujol mull. The notable intensity in the Raman, as well as the IR activity of the 299 cm^{-1} band, would argue against assigning it as ν_{13} ; nevertheless, the calculated scaled fundamental at 291.6 cm^{-1} (set BII, Table 8), only 8 cm^{-1} larger than the experimental datum, decided the final assignment.

B₁ Symmetry. The C–H wagging mode, ν_{14} , was assigned as the weak IR and Raman bands at 836 cm^{-1} . ν_{15} , representing the C–Cl wagging, was identified with the band at 507 cm^{-1} in the IR and Raman spectra. The characterization of the latter (Table 8) showed also contributions of ring torsions. The lowest B_1 fundamental, ν_{16} , was not taken into account to refine the scale factors, so the calculated wavenumber at 92 cm^{-1} was a prediction. This value is remarkably low for a mode describing C–Cl wagging and ring torsion movements. No similar behavior has been found in other dichlorodiazines or chlorobenzenes. Moreover, a risk exists in this spectral area—that some experimental bands can be associated with external rather than internal modes.⁶² ν_{16} could be identified as the Raman shoulder at 114 cm^{-1} , although the Raman band at 156 cm^{-1} could be another option. However, the latter alternative would present a deviation of 74 cm^{-1} from the calculated wavenumber (Table 8).

3,4,5-Trichloropyridazine. A' Symmetry. The C–H stretching mode, ν_1 , was assigned at 3069 cm^{-1} in the IR and at 3070 cm^{-1} in the Raman. The Raman spectra in HCCl_3 , CCl_4 , and CS_2 solutions gave 3075, 3074, and 3071 cm^{-1} , respectively, for this fundamental. The a priori spectra, sets AI, AII, BI, and BII, as well as the calculated quantum mechanical IR intensities, played a determining role in the assignment of the rest of the A' modes. The proposed assignment is shown in Table 9, where the characterization of each normal mode is also presented. In this trichlorinated molecule, all the modes appear significantly mixed with contributions of each kind of molecular displacement, C–Cl stretching and bending modes being the only exceptions. ν_{10} , ν_{12} , and ν_{13} , related to the bands at 826, 509, and 485 cm^{-1} , respectively, represented modes with major C–Cl stretchings contributions. Their wavenumbers agree with those

observed for the same modes in 1,3,5-trichlorobenzene.⁶² The first relatively pure C–Cl bending was assigned at 413 cm^{-1} in the IR and at 414 cm^{-1} in the Raman. The IR band in Nujol mull at 223 cm^{-1} and at 217 cm^{-1} in the Raman was identified with the next C–Cl bending mode, ν_{16} . Finally, ν_{17} , the third C–Cl in-plane deformation fundamental, was related to the band in the Raman at 211 cm^{-1} .

A'' Symmetry. The calculated and observed wavenumbers of the A'' fundamentals are shown in Table 9. The C–H wagging mode, ν_{18} , was assigned at 931 cm^{-1} . The rest of the fundamentals are characterized by ring torsions and C–Cl waggings contributions. As in 3,6-dichloropyridazine, the lowest fundamental, ν_{24} , was not considered in the refinement procedure of the scale factors. Thus, its calculated wavenumber at 76 cm^{-1} is a prediction. Bearing in mind the low calculated value for this fundamental, the same comments could be made as for the dichlorinated derivative. The Raman shoulder at 81 cm^{-1} was accepted as a possible assignment, although the Raman band at 112 cm^{-1} should be also considered, being only 36 cm^{-1} higher than the calculated wavenumber.

V. Conclusions

More reliable infrared and Raman spectra of 3,6-dichloropyridazine in various phases and solvents were recorded. Two Fermi resonances are proposed for both C–H stretching fundamentals which were corrected by the intensities method. The infrared records in mineral oil were decisive in assignment of the low-frequency normal modes. For the first time, the infrared and Raman spectra of 3,4,5-trichloropyridazine in various phases and solvents were taken. Similar to the dichlorinated derivative, the infrared spectra in mineral oil helped to identify the low-frequency modes.

Several quantum mechanical methods were used to predict the geometries of these two molecules. Bond angles were not very sensitive to the level of theory, although more significant differences were observed in the bond distances. The calculations support that the pyridazine and its chlorinated derivatives show less aromatic character than expected. First, the CCSD method with the 6-311G** basis set and second, the B3LYP exchange-correlation functional with the 6-31G* basis functions gave the most reliable structural parameters for both molecules.

The vibrational assignment was carried out taking into account the experimental evidence supported by a scaled quantum mechanical force field from a B3LYP/6-31G* calculation. Two series of scale factors were tested. The a priori spectra calculated from both of them were helpful in an initial assignment of the fundamentals. However, the scaling factors calibrated from pyridazine, instead of the standard scale factors derived from a training set of 30 organic molecules, proved to be necessary to resolve the most difficult spectral areas, particularly in those cases related to out-of-plane normal modes and with C–Cl displacements. These results emphasize that scale factors describing a particular electronic environment are more effective to explain the complete spectra of a series of related molecules.

Acknowledgment. G. P. thanks the OTKA Research Foundation of Hungary (Grant No. T-025830) for supporting part of this work. We also thank the Robert Welch Foundation for support of the work done in Austin.

References and Notes

- (1) Katritzky, A. R.; Scriven, E. V. S.; Charles, W. R. *Comprehensive Heterocyclic Chemistry II. The Structure, Reactions, Synthesis and Uses of Heterocycles. A Review of the Literature 1982–1995*; Pergamon Press: New York, 1996.

- (2) Joule, J. A.; Smith, G. F. *Heterocyclic Chemistry*; van Nostrand: Wokingham, 1987.
- (3) Barlin, G. B. *The Pyrazines*; Wiley-Interscience: New York, 1982.
- (4) Katritzky, A. R.; Charles, W. R. *Comprehensive Heterocyclic Chemistry. The Structure, Reactions, Synthesis and Uses of Heterocycles*; Pergamon Press: New York, 1984; Vol. 3.
- (5) (a) Shiroza, T.; Ebisawa, N.; Furihata, K.; Eudo, T.; Seto, H.; Otake, N. *Agric. Biol. Chem.* **1982**, *46*, 865. (b) Shiroza, T.; Ebisawa, N.; Furihata, K.; Shimazu, A.; Eudo, T.; Seto, H.; Otake, H. *S. N. Agric. Biol. Chem.* **1982**, *46*, 1885. (c) Shiroza, T.; Ebisawa, N.; Furihata, K.; Eudo, T.; Seto, H.; Otake, N. *Agric. Biol. Chem.* **1982**, *46*, 1891. (d) Huang, C. H.; Crooke, S. T. *Cancer Res.* **1985**, *45*, 3768. (e) Gries, J.; Schuster, J.; Giertz, H.; Lehmann, H. D.; Lenke, D.; Wortsmann, W. *Arzneim.-Forsch.* **1981**, *31*, 1533. (f) Lehmann, H. D.; Giertz, H.; Kretzschmar, R.; Lenke, D.; Phillipsborn, G.; Raschack, M.; Schuster, J. *Arzneim.-Forsch.* **1981**, *31*, 1544. (g) Lenke, D.; Gries, J.; Kretzschmar, R. *Arzneim.-Forsch.* **1981**, *31*, 1558.
- (6) (a) Karapetyan, N. V.; Rakhimberdieva, M. G.; Lehoczki, M.; Krasnovskii, A. A. *Biokhimiya* (Moscow) **1981**, *46*, 2082. (b) Kosáry, J.; Szilágyi, G.; Mátyus, P.; Csakó, K.; Kasztreiner, E. *Acta Pharm. Hung.* **1983**, *53*, 106. (c) Gribova, Z. P.; Tikhonov, A. N.; Postnov, L. A.; Kirbe, I.; Zoz, N. N. *Biofizika* **1985**, *30*, 1035. (d) Konečný, V.; Kovač, Š.; Varkonda, Š. *Chem. Zvesti.* **1984**, *83*, 239. (e) Konečný, V.; Kovač, Š.; Varkonda, Š. *Collect. Czech. Chem. Commun.* **1985**, *50*, 492. (f) Konečný, V.; Kovač, Š.; Varkonda, Š. *Chem. Zvesti.* **1985**, *39*, 513. (g) Ito, T.; Hosono, A.; Tachibana, H.; Nitani, K. *Nippon Nogei Kagaku Kaishi* **1983**, *57*, 445. (h) Yemia, A. A.; Doss, N. L.; Ismail, M. N. *Die Augenandte Makromolekulare Chemie* **1989**, *168*, 1. (i) Burrow, M. P.; Gray, G. W.; Lacey, D.; Toyne, K. J. *N. Chem.* **1986**, *26*, 21. (j) Tisler, M.; Stanovnik, B. *Adv. Heterocycl. Chem.* **1990**, *49*, 385.
- (7) Heinisch, G.; Frank, H. In *Progress in Medicinal Chemistry*; Ellis, G. P., West, G. B., Eds.; Elsevier: New York, 1990; Vol. 27, p 1.
- (8) (a) Kizuki, S.; Ishibashi, Y.; Shimada, H.; Shimada, R. *Memoirs of the Faculty of Science*; Kyushu University, Ser. C, **1981**, *13*, 7. (b) Anantharama Sarma, Y. *Spectrochim. Acta* **1974**, *30A*, 1801. (c) Nakama, S.; Shimada, H.; Shimada, R. *Bull. Chem. Soc. Jpn.* **1984**, *57*, 2584. (d) Gauthier, H.; Lebas, J. M. *Spectrochim. Acta* **1979**, *35A*, 787.
- (9) Kartha, S. B. *Can. J. Spectrosc.* **1982**, *27(1)*, 1.
- (10) Almennigen, A.; Bojornsen, G.; Ottersen, T.; Seip, R.; Strand, T. *G. Acta Chem. Scand.* **1977**, *A31*, 63–68.
- (11) Morrison, C. A.; Smart, B. A.; Parsons, S.; Brown, E. M.; Rankin, D. W. H.; Robertson, H. E.; Miller, J. J. *Chem. Soc., Perkin Trans.* **1997**, *2*, 857.
- (12) (a) Sanyal, N. K.; Srivastava, S. L.; Goel, R. K.; Sharma, S. D. *Proc. Indian Acad. Sci.* **1979**, *88*, 279. (b) Goel, R. K.; Sharma, S. N. *Indian J. Pure Appl. Phys.* **1979**, *17*, 630. (c) Mohan, S.; Murugan, R. *Indian J. Pure Appl. Phys.* **1993**, *31*, 496.
- (13) Terazina, M.; Yamavehi, S.; Hirota, N. *J. Chem. Phys.* **1976**, *84*, 3679.
- (14) Rauhut, G.; Pulay, P. *J. Phys. Chem.* **1995**, *99*, 3093.
- (15) Diem, M. *Introduction to Modern Vibrational Spectroscopy*; Wiley & Sons: New York, 1993.
- (16) Hehre, W. J.; Radom, L.; Schleyer, P. W. R.; Pople, J. A. *Ab Initio Molecular Orbital Theory*; Wiley: New York 1986.
- (17) Møller, C.; Plesset, M. S. *Phys. Rev.* **1934**, *46*, 618.
- (18) Seminario, J. M.; Polizer, P., Eds. *Modern Density Functional Theory. A Tool for Chemistry*; Elsevier: Amsterdam, 1995.
- (19) Becke, A. D. *Phys. Rev.* **1988**, *A38*, 3098.
- (20) Lee, C.; Yang, W.; Parr, R. G. *Phys. Rev.* **1988**, *B41*, 785.
- (21) Becke, A. D.; *J. Chem. Phys.*, **1993**, *98*, 5648.
- (22) (a) Ditchfield, R.; Hehre, W. J.; Pople, J. A. *J. Chem. Phys.* **1971**, *54*, 724. (b) Hehre, W. J.; Ditchfield, R.; Pople, J. A. *J. Chem. Phys.* **1972**, *56*, 2257.
- (23) Hariharan, P. C.; Pople, J. A. *Theor. Chim. Acta* **1973**, *28*, 213.
- (24) Lipkowitz, K. B.; Boyd, D. B., Eds. *Reviews in Computational Chemistry*; VCH: New York, 1991; Vol. 2.
- (25) Frisch, M. J.; Pople, J. A.; Binkley, J. S. *J. Chem. Phys.* **1984**, *80*, 3265.
- (26) Shavitt, I. In *Modern Theoretical Chemistry*; Shafer, H. F., Ed.; Plenum: New York, 1977; Vol. 3, p 189.
- (27) Scuseria, G. E.; Janssen, C. L.; Schaefer, H. F., III. *J. Chem. Phys.* **1988**, *89*, 7382.
- (28) (a) Scuseria, G. E. *Chem. Phys. Lett.* **1991**, *176*, 27. (b) Watts, J. D.; Gauss, J.; Bartlett, R. J. *J. Chem. Phys.* **1993**, *98*, 8718.
- (29) Pulay, P. *Mol. Phys.* **1969**, *17*, 197.
- (30) Frisch, M. J.; Trucks, G. W.; Head-Gordon, M.; Gill, P. M. W.; Wong, M. W. J.; Foresman, B.; Johnson, B. G.; Schlegel, H. B.; Robb, M. A.; Replogle, E. S.; Gomperts, R.; Andres, J. L.; Raghavachari, K.; Binkley, J. S.; Gonzalez, C.; Martin, R. L.; Fox, D. J.; Defrees, D. J.; Baker, J.; Stewart, J. J.; Pople, J. A. GAUSSIAN 92, revision E.3; Gaussian, Inc.: Pittsburgh, PA, 1992.
- (31) Frisch, M. J.; Trucks, G. W.; Schlegel, H. B.; Gill, P. M. W.; Johnson, B. G.; Robb, M. A.; Cheeseman, J. R.; Keith, T.; Petersson, G. A.; Montgomery, J. A.; Raghavachari, K.; Al-Laham, M. A.; Zakrzewski, V. G.; Ortiz, J. V.; Foresman, J. B.; Cioslowski, J.; Stefanov, B. B.; Nanayakkara, A.; Challacombe, M.; Peng, C. Y.; Ayala, P. Y.; Chen, W.; Wong, M. W.; Andres, J. L.; Replogle, E. S.; Gomperts, R.; Martin, R. L.; Fox, D. J.; Binkley, J. S.; Defrees, D. J.; Baker, J.; Stewart, J. P.; Head-Gordon, M.; Gonzalez, C.; Pople, J. A. GAUSSIAN 94, revision B.1.; Gaussian, Inc.: Pittsburgh, PA, 1995.
- (32) Stanton, J. F.; Gauss, J.; Watts, J. D.; Lauderdale, W. J.; Bartlett, R. J. *Int. J. Quantum Chem.* **1992**, *526*, 979.
- (33) Rauhut, G.; Pulay, P. *J. Am. Chem. Soc.* **1995**, *117*, 4167.
- (34) Baker, J.; Jarzecki, A. A.; Pulay, P. *J. Phys. Chem.* **1998**, *102*, 1412.
- (35) Scott, A. P.; Radom, L. *J. Phys. Chem.* **1996**, *100*, 16502.
- (36) Berezin, V. I. *Opt. Spektrosk.* **1965**, *18*, 71.
- (37) Chappel, P. J.; Ross, I. G. *J. Mol. Spektrosk.* **1977**, *66*, 192.
- (38) Fernández, M.; López, J. J.; Cardenete, A.; Arenas, J. F. *J. Mol. Struct.* **1986**, *142*, 33.
- (39) Innes, K. K.; Ross, I. G.; Moomaw, W. R. *J. Mol. Spectrosc.* **1988**, *132*, 492.
- (40) Arenas, J. F.; López-Navarrete, J. T.; Marcos, J. I.; Romero, J. J. *Opt. Pur. Apl.* **1989**, *22*, 103.
- (41) Wiberg, K. G. *J. Mol. Struct.* **1990**, *244*, 61.
- (42) Bérces, A. R.; Szalay, P. G.; Magdo, I.; Fogarasi, G.; Pongor, G. *J. Phys. Chem.* **1993**, *97*, 1356.
- (43) Billes, F.; Mikosch, H. *J. Mol. Struct.* **1995**, *349*, 409.
- (44) Billes, F.; Mikosch, H.; Holly, S. *J. Mol. Struct.* **1998**, *423*, 225.
- (45) Martin, J. M. L.; Van Alsenoy, C. *J. Phys. Chem.* **1996**, *100*, 6973.
- (46) Vázquez, J.; López González, J. J.; Márquez, F.; Boggs, James E. *J. Raman Spectrosc.* **1998**, *29*, 547.
- (47) Florian, J.; Johnson, G. B. *J. Phys. Chem.* **1994**, *98*, 3681.
- (48) Michalska, D.; Bienko, D. C.; Abkowitz-Bienko, A. J.; Zatajka, Z. *J. Phys. Chem.* **1996**, *100*, 17786.
- (49) Hedberg, L.; Mills, I. M. *J. Mol. Spectrosc.* **1993**, *160*, 117. ASYM20-ASYM40, version 3.0.
- (50) (a) Fogarasi, G.; Pulay, P. *Ab Initio Calculation of Force Fields and Vibrational Spectra*. In *Vibrational Spectra and Structure*; Durig, J. R., Ed.; Elsevier: Amsterdam, 1985; Vol. 14, p 125. (b) Fogarasi, G.; Zhou X.; Taylor, P. W.; Pulay, P. *J. Am. Chem. Soc.* **1992**, *114*, 8191.
- (51) (a) Pongor, G.; Fogarasi, G.; Magdo, I.; Boggs, J. E.; Keresztury, G.; Ignatyev, I. S. *Spectrochim. Acta* **1992**, *48A*, 111. (b) Pongor, G. Program SCALE3. Department of Theoretical Chemistry Eötvös Loránd University: Budapest, 1993.
- (52) Blake, A. J.; Rankin, D. W. H. *Acta Crystallogr., Sect. C* **1991**, *C47*, 1933.
- (53) Johnson, B. G.; Gill, P. W. M.; Pople, J. A. *J. Chem. Phys.* **1993**, *98*, 5612.
- (54) Craddock, S.; Purves, C.; Rankin, D. W. H. *J. Mol. Struct.* **1990**, *220*, 123.
- (55) Werner, W.; Dreizler, H.; Rudolph, H. D. *Z. Naturforsch.* **1967**, *A22*, 531.
- (56) Wiberg, K. B.; Nakaji, D.; Breneman, C. M. *J. Am. Chem. Soc.* **1989**, *111*, 4178.
- (57) (a) Blake, A. J.; Brain, P. T.; McNab, H.; Miller, J.; Morrison, C. A.; Parsons, S.; Rankin, D. W. H.; Robertson, H. E.; Smart, B. A. *J. Phys. Chem.* **1996**, *100*, 12280. (b) Brain, P. T.; Morrison, C. A.; Parsons, S.; Rankin, D. W. H. *J. Chem. Soc., Dalton Trans.* **1996**, 4589.
- (58) Koput, J. *Chem. Phys. Lett.* **1995**, *240*, 553.
- (59) Califano, S. *Vibrational States*; Wiley-Interscience: London, 1976.
- (60) Fermi, E. Z. *Physik.* **1931**, *71*, 251.
- (61) (a) Mckean, D. C. *Spectrochim. Acta* **1973**, *29A*, 1559. (b) Hill, I. R.; Levin, I. W. *J. Chem. Phys.* **1979**, *70*, 842.
- (62) Zhou, X.; Fogarasi, G.; Liu, R.; Pulay, P. *Spectrochim. Acta* **1993**, *49A*, 1499.
- (63) Ito, M.; Shigeoka, T. *J. Chem. Phys.* **1966**, *44*, 1001.